PHYSICAL REVIEW B VOLUME 22, NUMBER 8 15 OCTOBER 1980

Pressure dependence of the Raman modes and pressure-induced phase changes in $CuGaS_2$ and $AgGaS_2$

C. Carlone,* D. Olego, A. Jayaraman,† and M. Cardona
Max-Planck-Institut für Festkörperforschung, 7000 Stuttgart 80, Federal Republic of Germany
(Received 18 June 1980)

The pressure dependence of the Raman peaks of $CuGaS_2$ and $AgGaS_2$ (chalcopyrite structure) has been studied up to 20 GPa in a gasketed diamond anvil cell. Nonlinear pressure dependence of several phonon frequencies have been noted, including a softening of the lowest Γ_5 phonon, prior to a phase transition, which takes place at 16.5 ± 0.5 GPa in $CuGaS_2$ and 4.2 ± 0.5 GPa in $AgGaS_2$. In the latter material, discontinuous changes of the Raman frequencies indicate another phase transition at 11.6 ± 0.5 GPa. The transition in $CuGaS_2$ is believed to be to the disordered rocksalt structure, and in $AgGaS_2$, the high-pressure transition is to the rocksalt, or to the closely related α-$NaFeO_2$ structure. In $AgGaS_2$, the softening of the lowest Γ_5 phonons can be followed across the 4.2-GPa phase transition, an observation which to our knowledge has been made for the first time in a tetrahedral semiconductor. It is concluded that the first phase transition takes place in all these materials whenever the lowest Γ_5 mode (or its equivalent) is lowered to 0.7 times its zero-pressure value. The effect of pressure on the phonon frequencies is discussed in terms of Born's transverse dynamical charges and their pressure dependence.

INTRODUCTION

The I-III-VI_2 compounds are isoelectronic with the zinc-blende II-VI compound semiconductors and crystallize in the chalcopyrite structure,[1] which may be regarded as a superlattice of the zinc-blende type. Because of this special relationship, the properties of the I-III-VI_2 compounds are, in general, similar to their binary II-VI analogs. High-pressure studies[2,3] on ternary semiconductors have shown that the chalcopyrite structure becomes unstable under pressure and transforms either to the NaCl-type structure or to a distorted version of it with rhombohedral symmetry (α-$NaFeO_2$ type[3]). In some cases, a chemically disordered zinc-blende phase has also been seen in pressure-quenched products.[3] Usually, a phase transition occurs because of a lattice instability or soft mode, and in this connection a study of the phonon behavior is both useful and revealing. It has been shown by Raman spectroscopy in several III-V and II-VI compounds that the low-frequency mode softens[4,5] and thus exhibits a negative-mode Grüneisen parameter γ_i. In fact a relationship between γ and transition pressure seems to exist.[6]

We undertook a Raman study of two typical ternary compounds, $CuGaS_2$ and $AgGaS_2$ under high pressure, firstly to investigate the lattice instabilities in them by following the Raman modes and secondly to see how their lattice dynamics are influenced by pressure. A pressure study on $CuGaS_2$ up to 0.7 GPa (Ref. 7) has indicated a negative Grüneisen parameter for the lowest Γ_5 mode. The pressure range of this study,[7] however, was quite inadequate to be anywhere near the expected phase-transition pressure.

The choice of $CuGaS_2$ and $AgGaS_2$ for our Raman studies was dictated by the transparency of the above two crystals in the visible spectrum which leads to adequate scattering intensity within the diamond cell. Further, these materials have been studied rather extensively, both by Raman scattering and by infrared absorption at ambient pressure[8-10] and the observed Raman peaks interpreted on the basis of lattice dynamics appropriate for their crystal symmetry.

In this study, we have been able to extend measurements up to 20 GPa. Our results lead to a slight revision of some of the previous assignments of the Raman frequencies for $CuGaS_2$. The almost negligible effect of pressure on the LO-TO splittings suggests no significant changes with pressure of the dynamical charges on the ions concerned. We have also observed in $AgGaS_2$ an interesting mode-softening behavior which is presumably connected with a phase transition as the transition is approached from either side. The slope of this mode above the phase transition is roughly double that below, a fact which is easy to account for with a modified soft-mode theory. Our study reveals that the Raman data provide a sensitive tool to probe pressure-induced phase transitions in tetrahedral materials. Examining these and other existing data, we find that the first phase transition takes place when the lowest, soft transverse zone-boundary phonon of a zinc blende, or its equivalent Γ phonon of a chalcopyrite, is lowered to ~0.7 of its original frequency.

EXPERIMENTS

Our samples were cut from single crystals of $CuGaS_2$ and $AgGaS_2$, grown at Bell Laboratories and

kindly given to us by Dr. B. Tell. Extensive optical studies including Raman scattering have been reported on materials from the same batches. The results of these studies as well as the method of preparation of the crystals have been discussed in several papers and in the monograph by Shay and Wernick.[1] For light scattering measurements under pressure, very thin slices (30–40 μm in thickness) were polished and tiny platelets, 50 to 100 μm in linear dimensions from these slices, were used. The $CuGaS_2$ samples were light orange in color and the $AgGaS_2$ were light yellow. The latter crystals were slightly doped with lithium and appeared yellow-green in large thicknesses.

A gasketed diamond anvil cell[5] with sapphire backing, such as the one described by Syassen and Holzapfel,[11] was employed for Raman studies under pressure. The gasket was made from heat-treated Inconel. Its thickness was 100–120 μm and the diameter of the aperture in the gasket 200 μm. A 4:1 methanol-ethanol mixture served as the pressure medium. For pressure calibration, a tiny ruby chip was placed inside the cell along with the sample. The backscattering geometry, as described by Weinstein and Piermarini,[5] was adopted for the diamond cell. The green line of the argon ion laser at 514.5 nm and the 568.1-, 647.1-, and 676.4-nm lines of the krypton laser were used as exciting radiation. The Raman spectra were obtained using a Spex model 1402 double monochromator provided with a cooled RCA C 31034 photomultiplier and standard photon counting system. All measurements were carried out at room temperature.

RESULTS

The pressure dependence of the Raman peaks for $CuGaS_2$ is shown in Fig. 1. At 16.5 ± 0.5 GPa the crystal became black, evidently due to a phase change. For the high-pressure black phase, no Raman peaks were observed. In Table I on the left side, we compare our results obtained with a large cyrstal at ambient pressure with the results of other investigators.[8,9] On the right-hand side, the values of the coefficients a, b, and c used in fitting the high-pressure data to the polynomial

$$\omega = \omega_0 + ap + bp^2 + cp^3 \qquad (1)$$

are given. In the last column we have given the values of the mode Grüneisen parameters $\gamma_i = -\partial \ln\omega_i / \partial \ln V$, where ω_i is the phonon frequency and V the crystal volume, which was obtained by using the Murnaghan equation of state, with a bulk modulus $B_0 = 940 \pm 150$ kbar and $B' = 4.3$. The present γ values are compared with those of Bettini and Holzapfel[7] up to 0.7 GPa.

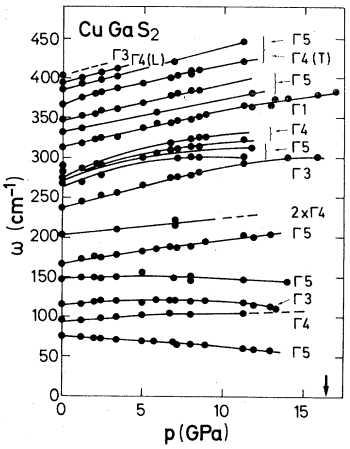

FIG. 1. The pressure dependence of the Raman peaks in $CuGaS_2$. All the phonons, except the one at 401 cm^{-1}, could be followed as a function of pressure. The broad feature in the Raman spectrum between 270 and 290 cm^{-1} at $p = 0$ (four dots in the figure) can be resolved into four components by use of resonance Raman scattering (Ref. 10). The assignment on some of the phonons has been changed from previous work (see Table I). The arrow at 16.5 GPa indicates the change of phase.

Analogous data for $AgGaS_2$ are shown in Table II while Fig. 2 shows the shift of the Raman peaks in $AgGaS_2$ with pressure. From Fig. 2, it appears that there is a phase change at about 4.2 ± 0.5 GPa, as evidenced by the appearance of two new Raman lines. Further, the lowest Γ_5 mode exhibits softening and a new mode emerges at higher pressures. This behavior is shown in more detail in Fig. 3. At about 11.6 ± 0.5 GPa, evidence for yet another phase change is seen. Near this pressure, the sample turns black when observed visually with a microscope. A few Raman peaks are still observed for this black phase. In Table III and IV, the values of the constants used in the polynomial are given, along with the mode Grüneisen-parameter γ values for the two high-pressure phases.

In the case of $CuGaS_2$, we observed a marked broadening of the Γ_1 mode (312 cm^{-1} at ambient pressure). The half-width Γ as a function of pressure is plotted for this mode in Fig. 4. The Γ_1 mode is the strongest peak in the Raman spectrum, as obtained in the pressure cell. It is possible that the broadening may indicate some pressure-induced atomic displacements, or even cationic disordering prior to the phase transition.

DISCUSSION

Chalcopyrite has the symmetry $D_{2d}^{12} - I\bar{4}2d$ and the body-centered tetragonal unit cell contains four formula units. A total of 24 modes are possible

TABLE I. Pressure data for the Raman-active phonons of $CuGaS_2$ (the units of a, b, and c are such that ap, bp^2, and cp^3 are in cm^{-1}, where p is in kilobars).

$CuGsS_2$ Mode symmetry	$\omega = \omega_0 + ap + bp^2 + cp^3$ $\omega_0(cm^{-1})$ Ref. 8	Ref. 9	Ref. 7	Present work	$a \times 10^{-2}$ ±5%	$b \times 10^{-4}$ ±10%	$c \times 10^{-6}$ ±15%	γ Ref. 7	Present work
	75	74	74	75	−6.4	−3.1	−1.6	−0.65 ±0.4	−0.80±0.2
$\Gamma_{5T,L}$	76			75					
	259	95	94	95	+20	−6.0	−3.0	+0.8 ±0.4	+2.0 ±0.4
$\Gamma_{4T,L}$	284	95		95					
	138	97	97	116	+15.7	−12			+1.3 ±0.3
Γ_3									
	95	not	not	147	+12.8	−10			0.8 ±0.2
$\Gamma_{5T,L}$	98	assigned	assigned	147					
	147	156	165	167	+34.9	−3.6		1.5 ± 0.3	2.0 ± 0.5
$\Gamma_{5T,L}$	167	160		167					
Second order				203	+23.6				1.1 ± 0.2
Γ_3	203	203	not assigned	238	+56.0	−6.0	−2.0		2.6 ± 0.6
$\Gamma_{5T,L}$	260	262	258	273	+41.7	−8.0	−6.0		1.4 ± 0.3
	278	276		283	+33	−3.0	−1.0		1.1 ± 0.2
$\Gamma_{4T,L}$	339	262	277	286	+31.9	−4.0	−2.0		1.1 ± 0.2
	369	281		288	+51.0	−9.0			1.7 ± 0.3
Γ_1	312	312	312	312	+48.3	−2.0	−0.8	+1.8 ± 0.2	1.5 ± 0.3
$\Gamma_{5T,L}$	335	332	332	332	+41.4				1.2 ± 0.2
	352	352	349	347	+54.2			1.5 ± 0.2	1.5 ± 0.3
Γ_3	243	358	358	401					
$\Gamma_{4T,L}$	371	368	349	367	+56.3	−9.0		1.6 ± 0.2	1.5 ± 0.3
	402	401	366	393	+59				1.4 ± 0.3
$\Gamma_{5T,L}$	365	363	364	367	+56.3	−9.0		1.6 ± 0.2	1.5 ± 0.3
	387	384	366	385	+51.7			1.3 ± 0.2	1.3 ± 0.3
								$B_0 = 940 \pm 150$ kbar	
								$B' = 4.3 \pm 0.3$	

TABLE II. Pressure data for the Raman-active phonons of $AgGaS_2$ (the units of a, b, and c are such that ap, bp^2 and cp^3 are in cm^{-1}, where p is in kilobars).

$AgGaS_2$ Mode symmetry	$\omega_0(cm^{-1})$ Ref. 8	$\omega_0(cm^{-1})$ Ref. 9	$\omega=\omega_0+ap+bp^2+cp^3$ Present	$a\times10^{-2}$	$b\times10^{-4}$	$c\times10^{-6}$	γ Present work
Γ_{5T}	63	34	36	−26	−40		−4.4
Γ_{5L}	64	34	36				
Γ_{4T}	195	65	65	0	0		
Γ_{4L}	199	66	65				
Γ_3	118	54					
			125				
Γ_{5T}	93	95	96	+8.3	−30	−2.0	0.52
Γ_{5L}	98	95					
Γ_{5T}	158	157	160	+10.8	−11		0.41
Γ_{5L}	160	160	161	+15.0	−76		0.56
Γ_3	179	190					
Γ_{5T}	225	226	213	+53.0	−4.0	−10	1.49
Γ_{5L}	230	232	224	+93.0	−24	−10	2.49
Γ_{4T}	215	212	213	+53.0	−4.0	−10	1.49
Γ_{4L}	239	238	215	+73.0	−4.0		1.79
Γ_1	295	295	293	50.0	−40		1.02
Γ_{5T}	327	325					
Γ_{5L}	347	349					
Γ_3		334					
Γ_{4T}	366	367	367	52.0			0.85
Γ_{4L}	340	399					
Γ_{5T}	368	368					
Γ_{5L}	392	398	392	53.0			0.81
Second order			517	107	a		1.25
							$B_0{}^b = 600 \pm 100$ kbar

[a] The second order phonon has a kink at about 70 kbar, which is associated with the change of phase.

[b] This value is derived from the elastic constants given in Ref. 1.

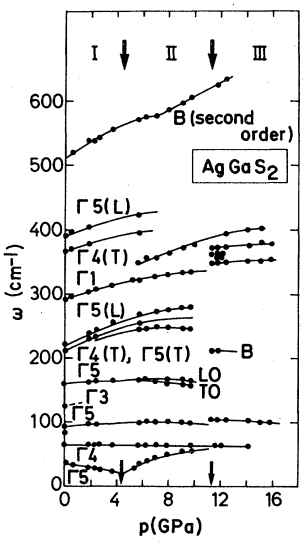

FIG. 2. The pressure dependence of the Raman peaks in $AgGaS_2$. Phase change at 4.2 GPa and at 11.6 GPa are indicated by arrows. B stands for broad line.

for the two formula units contained in the primitive cell. The representation Γ at the center of the zone is reducible into

$$\Gamma = 1\Gamma_1 + 2\Gamma_2 + 3\Gamma_3 + 4\Gamma_4 + 7\Gamma_5 , \tag{2}$$

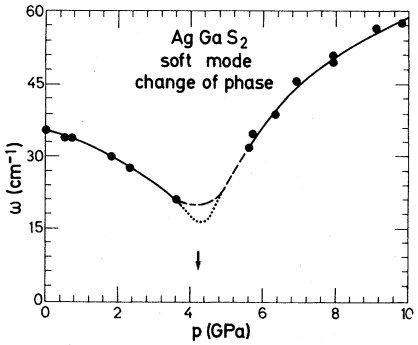

FIG. 3. The softening of the lowest Γ_5 phonon in $AgGaS_2$ across the phase change at 4.2 GPa. The dashed and dotted lines are hypothetical curves at the critical point.

TABLE III. Data for phase-II data of $AgGaS_2$. From Fig. 3, $p_{II}=42$ kbar. The high value of γ (35) results from its estimation near the critical pressure where the slope is very large and ω_0 small.

$AgGaS_2$ phase II	ω_0	$\omega=\omega_0+a(p-p_{II})+b(p-p_{II})^2+c(p-p_{II})^3$ $a\times10^{-2}$	$b\times10^{-4}$	$c\times10^{-6}$	γ
	17	105	−15	−10	35
	335	92	−7	−7	1.6
					$B_0=600$ kbar

of which $1\Gamma_4$ and $1\Gamma_5$ are acoustic. The symmetry and activity of the normal modes have been given.[8,9,12] With the splitting into transverse and longitudinal components for the ir-active modes of Γ_4 and Γ_5 symmetry, one expects 22 Raman-active phonons. We have been able to measure the pressure dependence of all but one of the 22 Raman modes in the case of $CuGaS_2$. We only observed 17 of these phonons for $AgGaS_2$. In the case of $CuGaS_2$, the pressure study has helped in removing some inconsistencies in previous assignments as discussed below. In Table I we have listed, in the order of increasing frequency shifts, the present assignment. The main regions where reassignment was felt necessary were (1) the Raman peaks at 147 and 167 cm^{-1} and (2) the broad unresolved region, observed between 270 and 290 cm^{-1} at ambient pressure. The 147-cm^{-1} component was not observed by Koschel and Bettini,[9] while Van der Ziel *et al.*[8] observed this component and grouped it with 167 cm^{-1} as a Γ_{5T}-Γ_{5L} pair. We believe that the 147 cm^{-1} and the 167 cm^{-1} represent two different Γ_5 modes, with negligible LO-TO splitting. It will be shown later why such an assignment is reasonable. With regard to the broad feature between 270 and 290 cm^{-1}, pressure work has enabled us to resolve them into four components as they begin to separate at high pressure (see Fig. 1). We have labeled the 273- and 283-cm^{-1} peaks as $\Gamma_{5L,T}$ and the 286 and 288 cm^{-1} as $T_{4T,L}$, respectively. We believe the grouping in the fifth column in Table I leads to the best possible overall agreement, considering the effect of pressure on the LO-TO splittings and reasonable values for the transverse dynamical charges of the ions. We now discuss the transverse dynamical charges and the effect of pressure on them.

DYNAMICAL CHARGE ON THE IONS

The LO-TO splitting $\omega_L-\omega_T$ of an ir-active mode can be represented phenomenologically by Born's transverse dynamical charges.[13] The theory can be generalized to a primitive cell with more than two atoms to yield

$$\omega_L^2-\omega_T^2=\frac{4\pi N}{\epsilon_\infty}\sum_i\left(\frac{e_i\hat{n}_i}{M_i^{1/2}}\right)^2, \tag{3}$$

where $1/N$ is the volume of the primitive cell, ϵ_∞ the infrared dielectric constant for frequencies well above the highest ω_L and below the electronic absorption edge, e_i the transverse dynamical charges on the atom, M_i the atomic mass, and $\hat{n}_i$ are the eigenvectors of the ir-active modes under consideration. Unfortunately we do not have the eigenvectors for $CuGaS_2$, but the eigenvectors worked out by Bettini[12] for $ZnGeP_2$ should be close enough for a reasonable estimate of the charges.

TABLE IV. Data for phase III of $AgGaS_2$. From Fig. 2, $p_{III}=116$ kbar. $B_0=1000$ kbar is estimated from Murnaghan's equation with $B_0=600$ kbar and $B_0'=4$.

$AgGaS_2$ phase III	ω_0	$\omega=\omega_0+a(p-p_{III})+b(p-p_{III})^2+c(p-p_{III})^3$ $a\times10^{2}$	$b\times10^{-4}$	$c\times10^{-6}$	γ
Acoustic type	106	−16.9	+17		−1.6
Second order of 106	211	−30 ± 15			−1.4
Optical type	350	+8.5			0.24
Optical type	358	+24 ± 10			0.66
Optical type	363	+24 ± 15			0.66
Optical type	373	+16			0.43
					$B_0=1000$ kbar

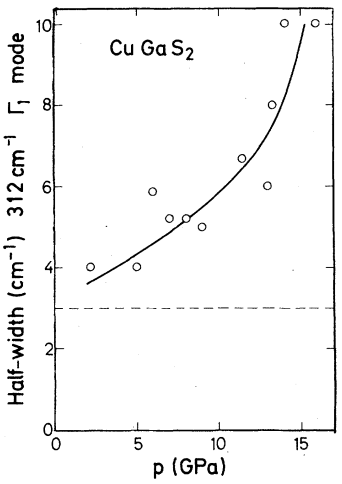

FIG. 4. The full width at half maximum for the 312 $cm^{-1}\Gamma_1$ mode of $CuGaS_2$ as a function of pressure. This effect may arise from pressure-induced atomic displacements prior to the phase transition.

The dynamical charges of the various ions *will be assumed*, for the time being, to be independent of the ir mode under consideration.

The dynamical charges for a given tetrahedral bond can be calculated from the bond-orbital model for tetrahedral semiconductors.[14] This model gives

$$e_T = -\Delta Z + \tfrac{20}{3}\alpha_P - \tfrac{8}{3}\alpha_P^3, \qquad (4)$$

where ΔZ is one-half the difference in core charges between the anion and the cation and α_p is the polarity or ionicity of the bond, as defined by Harrison.[14] The polarity of the I-VI bond was estimated as the average of those of the I-VII and of the II-VI bonds given by Harrison. A similar procedure was used for the III-VI bonds (see Table V).

In Table V we give the dynamical charges e_T calculated using Eqs. (3) and (4). The charges were obtained firstly by a fitting procedure using Eq. (3) to give the best possible agreement with the observed LO-TO splitting for Γ_4 and Γ_5 peaks, and then averaging the two sets of values. The charge e_T of sulfur was set equal to $-(e_{Cu}+e_{Ga})/2$ to ensure charge neutrality. The charges thus obtained for Cu, Ga, and S were put back into Eq. (3) and the splittings recalculated for the $3\Gamma_4$ and $5\Gamma_5$ modes (in column 3, Table V). Also, the net charges were calculated independently using Eq. (4). In the latter case, the ΔZ was given the value of 1.5 for the GaS bond and 2.5 for the CuS, and the α_p values were estimated as 0.625 and 0.74 for the two bonds, respectively, from the tables of values given in Ref. 14, p. 150. The LO-TO splittings calculated using the charges obtained from the bond-orbital model are shown in column 4 of Table V. In column 2, the experimentally observed splittings are given. The agreement between the latter and the calculated ones appears reasonable, as does the agreement between the charges e_T from the fit with Born's model and those estimated with the bond-orbital model. If one takes 147 and 167 cm^{-1} as a Γ_5 pair,[8] the LO-TO splitting of 20 cm^{-1} would lead to high values for e_T in Eq. (3). At higher pressures this would lead to even higher, unacceptable values for the charges. For these reasons we have changed the assignment of these two frequencies (see Table I).

The LO-TO splittings do not seem to change significantly, even over a large range of pressure. We conclude from this that there is negligible charge transfer under pressure.

TABLE V. LO-TO splittings of the Γ_4 and Γ_5 modes (ordered according to energy) and calculations with adjustable dynamical charges and with charges obtained from the bond-orbital model.

LO-TO splittings	Experimental	Dynamical charge $e_S = -1.55$ $e_{Cu} = +1.50$ $e_{Ga} = +1.60$	Bond orbital $e_S = -1.7$ $e_{Cu} = +1.4$ $e_{Ga} = +2.0$
Γ_4	0	0.2	2
	2	1.0	1
	26	25	31
Γ_5	0	0	0
	0	0.01	0.5
	0	0.01	0.5
	5	2	2
	10	5	6
	18	25	30

GRÜNEISEN PARAMETERS

The Grüneisen parameter for the lowest Γ_5 mode remains negative and its magnitude increases right up to the transition pressure. We find at zero pressure a value of -0.80 ± 0.2 for $CuGaS_2$, compared to the value of -0.65 ± 0.4 reported by Bettini and Holzapfel.[7] The negative γ value for the lowest Γ_5 mode can be related to the negative γ values for the transverse acoustic modes at the zone boundary in binary compounds with the zinc-blende structure. Therefore this mode in chalcopyrite has to be linked to the X_{5ac} zinc-blende mode. The latter compounds undergo a pressure-induced transition to a denser structure and negative γ characterizes the lattice instability in these. In the same manner, the negative γ value for the lowest Γ_5 mode in chalcopyrite structure forewarns the imminence of a phase transition in these compounds. In Fig. 5 we have added to the plot by Trommer *et al.*[6] of γ versus transition pressure for the III-V and II-VI compounds, the present result for $CuGaS_2$. The latter follows the general trend. $AgGaS_2$ on the other hand has a much larger negative $\gamma(\Gamma_5) = -4.4$ and does not fit into the picture. However, if one estimates the percentage softening of the frequency of the mode before the phase transition occurs, the value of 0.6 for $AgGaS_2$ is within the results noted for the other compounds (see Table VI).

SOFT-MODE BEHAVIOR OF $AgGaS_2$

The soft-mode behavior presented in Fig. 3 for $AgGaS_2$ bears a striking resemblance to mode softening observed in many systems as the temperature is varied through a phase-transition temperature T_c. The transitions of this type are usually second order and are describable by an order parameter ϕ which appraoches 0 at T_c. In structural transitions, however, ϕ measures the amount of change in atomic configuration from the old structure. In these transitions the structure of the new phase is uniquely determined by the eigenvector of the soft mode and the structure of the old phase.

In our case (see Fig. 3), there is a critical pressure P_c for the transition and the order parameter should therefore be pressure dependent. We have plotted in Fig. 6 ω^2 against pressure, in the hope of seeing a relationship of the form $\omega^2 = A + B(P_c - P)$ for $P < P_c$ and $\omega^2 = A + mB(P - P_c)$ for $P > P_c$. The solid line is the fit with this law to the

TABLE VI. Ratio R of the observed lowest Γ_5 frequency immediately before change of phase to that at atmospheric pressure.

Compound	R	Reference
ZnTe	0.7	4
Si	0.7	5
ZnSe	0.7	4
ZnS	0.7	4
$CuGaS_2$	0.76	this work
GaP	0.6	16
InP	0.77	6
GaAs	0.65	17
$AgGaS_2$	0.6	this work

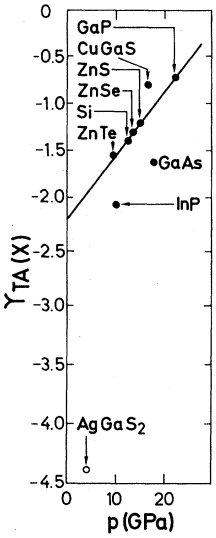

FIG. 5. The Grüneisen parameter of the Γ_5 mode that undergoes softening in group IV elements and III–V, II–VI, and chalcopyrite-structure compounds plotted as a function of the phase-transition pressure. Note that $AgGaS_2$ does not lie on the solid line.

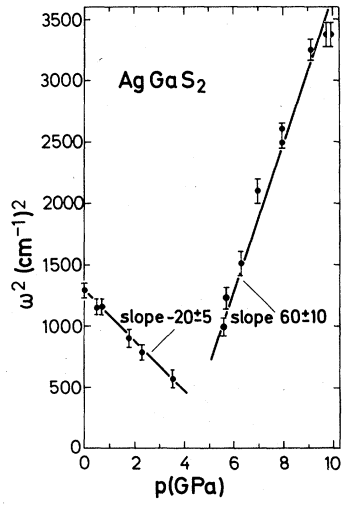

FIG. 6. ω^2 versus pressure for the soft Γ_5 mode in $AgGaS_2$. According to theory, the ratio of the slope above the phase change to that below the phase change should be 2; the experimental value of 3 ± 1 fits the theory only in the limit of error.

data. The ratio m of the slopes above and below P_c is found to be 3 ± 1, somewhat larger than the value $m = 2$ expected in a Landau-type second-order phase-transition model (although within the experimental error, it agrees marginally with $m = 2$). Nevertheless, we feel the behavior is indicative of a second-order transition among the closely related structures which may involve a simple distortion or disordering. Both these possibilities exist in the case of $AgGaS_2$.

Among the ternary compounds with the chalcopyrite structure, the tetragonal distortion is rather large for the silver compounds[1,8] and smaller for the copper compounds.[1,3] An additional distortion lowering the tetragonal symmetry would be needed to explain the Landau-type behavior of Fig. 3. Also, cationic disorder may be responsible for the transition. In this case, the tetragonal distortion would vanish and the chalcopyrite would turn into a chemically disordered zinc-blende type. Only very careful high-pressure x-ray single-crystal studies can unravel the situation.

PHASE TRANSITIONS IN I-III-VI_2 COMPOUNDS

From previous high-pressure studies[2,3] on $AgInTe_2$, $AgInSe_2$, $AgInS_2$, $AgGaSe_2$, and $CuInSe_2$, it has been shown that three high-density phases are possible for these compounds. They are (1) the high-density rhombohedral α-$NaFeO_2$ type, (2) the disordered rocksalt-type, and (3) the disordered zinc-blende phase. Of these, the α-$NaFeO_2$-type and the rocksalt-type have very nearly the same density, while the density of the zinc-blende phase is close to that of the chalcopyrite phase. The difference between α-$NaFeO_2$ and rocksalt (NaCl-type) is principally that the cations in the former are ordered, while they are disordered in the latter. Again the difference between the chalcopyrite and zinc-blende type has the same origin; in the zinc blende the cations are disordered as opposed to ordered cations in chalcopyrite. The sequence of phase transformations, namely, chalcopyrite → zinc blende → rocksalt has been seen in $AgInSe_2$ with increasing pressure at room temperature. However, at temperatures above 150°C, the pressure-quenched product from 3 GPa is found to have the α-$NaFeO_2$ structure. $AgInTe_2$ transforms directly to the rocksalt-type under room-temperature compression as well as at higher temperatures. Both the α-$NaFeO_2$ and rocksalt phases revert to the parent structure with time. An observation of interest in this connection is that the α-$NaFeO_2$ phase of $AgInSe_2$ when left at ambient pressure and temperature reverts to the rocksalt type, which then converts to the zinc-blende phase, before finally returning to the chalcopyrite structure.[2,3] Heating of the quenched product accelerates the reversion rate.

A radius ratio argument has been proposed for the pressure-induced phase transformations[2] for Ag- and Cu-based I-III-VI_2 compounds. If the R_c/R_a (where R_c is the averaged cationic radius and R_a the anionic radius) is much smaller than 0.414, the transformation would be to the rocksalt-type and, in the opposite case, it would be to the α-$NaFeO_2$ structure. This criterion would definitely rule out a transition to the α-$NaFeO_2$ structure for the $CuGaS_2$ whose $R_c/R_a = 0.378$. Hence we believe that the high-pressure transition near 16.5 GPa in $CuGaS_2$ is to the rocksalt-type. Absence of any Raman peaks in the black phase would be consistent with this. However, for $AgGaS_2$, R_c/R_a is 0.481 and we cannot rule out the α-$NaFeO_2$ phase. Since we observe a few Raman peaks even in the black phase of $AgGaS_2$ (above 12.0 GPa), the high-pressure phase could be α-$NaFeO_2$ or it may be a mixture of α-$NaFeO_2$ and rocksalt. In $AgInSe_2$ whose R_c/R_a is 0.492, both phases are present in the stability diagram. It may be noted here that the α-$NaFeO_2$ and rocksalt are closely related and both involve a drastic change in bonding when transforming from the tetrahedrally coordinated chalcopyrite structure.

SUMMARY AND CONCLUSIONS

The following conclusions have been reached as a result of this paper:

(1) The changes in the Raman peaks with pressure, clearly establish a phase transition near 16.5 GPa in $CuGaS_2$, possibly to the rocksalt structure and two phase transitions in $AgGaS_2$, one near 4.2 GPa and another near 11.6 GPa. We believe the upper transition in $AgGaS_2$ to be to the α-$NaFeO_2$ (or possibly to the rocksalt + α-$NaFeO_2$). The transition near 4.2 GPa is probably a subtler transition due to a change of symmetry which may or may not involve disordering of cations.

(2) The softening and negative Grüneisen parameter for the lowest Γ_5 mode in both $CuGaS_2$ and $AgGaS_2$ is well established. It seems to be related to the lattice instability leading to the observed phase transition in chalcopyrite-structure compounds.

(3) The phonon anomaly associated with the lowest Γ_5 mode in $AgGaS_2$ near 4.2 GPa is to our knowledge the first observation of phonon softening in tetrahedral semiconductors when a phase transition is approached from either side of the phase boundary.

(4) The LO-TO splittings and the negligible effect of pressure on them suggest no significant charge transfer on increasing pressure.

(5) We have applied the Born's transverse bond-charge model for calculating the charges on the ions. To achieve maximum consistency, we had to revise somewhat the previous assignments of the Raman frequencies.

(6) It is likely that the broadening of the Γ_1 mode in $CuGaS_2$ (see Fig. 4) may arise from pressure-induced atomic displacements prior to the phase transition. Such effects have been noted in $AgInSe_2$ in earlier studies.[15]

To establish the nature of the phase transitions, high-pressure x-ray studies on $CuGaS_2$ and $AgGaS_2$ are needed. Also, optical absorption studies on both systems could reveal the corresponding changes in the electronic structure. We propose to cary out these investigations in the near future. In conclusion, Raman studies under pressure are a powerful tool to probe pressure-induced phase transitions and can throw light on the microscopic mechanism behind the lattice instabilities.

ACKNOWLEDGMENTS

It is a pleasure to thank Dr. B. Tell for the samples. We wish to thank Dr. H. D. Hochheimer for his interest in this study and Mr. Dieterich for help in loading the high-pressure cell and Mr. Kisela for polishing the samples. We also benefited from the assistance rendered by Mr. Siemers and Mr. Wurster in the Raman lab. One of the authors, C. C., would like to thank the DAAD for financial support. A. J. would like to thank the Alexander von Humboldt Foundation for the U. S. Senior Scientist award.

---

*Permanent address: Université de Sherbrooke, Sherbrooke, Québec, Canada.

†Permaent address: Bell Laboratories, Murray Hill, N. J. 07974.

[1]J. L. Shay and J. H. Wernick, *Ternary Chalcopyrite Semiconductors Growth, Electronic Properties and Applications* (Pergamon, New York, 1975).

[2]A. Jayaraman, P. D. Dernier, H. M. Kasper, and R. G. Maines, High Temp.-High Pressures 9, 97–102 (1977).

[3]K. J. Range, G. Engert, and A. Weiss, Solid State Commun. 7, 1749 (1969) and papers cited therein.

[4]B. A. Weinstein, Solid State Commun. 24, 595 (1977).

[5]B. A. Weinstein and G. J. Piermarini, Phys. Rev. B 12, 1172 (1975).

[6]R. Trommer, H. Müller, M. Cardona, and P. Vogl, Phys. Rev. B 21, 4869 (1980).

[7]M. Bettini and W. B. Holzapfel, Solid State Commun. 16, 27–30 (1975).

[8]J. P. van der Ziel, A. E. Meixner, H. M. Kasper, and J. A. Ditzenberger, Phys. Rev. B 9, 4286 (1974).

[9]W. H. Koschel and M. Bettini, Phys. Status Solidi B 72, 729 (1975).

[10]S. Sugai, J. Phys. Soc. Jpn. 43, 5992 (1977).

[11]K. Syassen and W. Holzapfel, Phys. Rev. B 18, 5826 (1978).

[12]M. Bettini, Ph.D. thesis, University of Stuttgart, 1974 (unpublished).

[13]M. Born and K. Huang, *Dynamical Theory of Crystal Lattices* (Clarendon, Oxford, 1954), Chap. 2.

[14]W. Harrison, *Electronic Structure and the Properties of Solids* (Freeman, San Francisco, 1980), pp. 222–224.

[15]A. Jayaraman, B. Tell, and R. G. Maines, Appl. Phys. Lett. 32b, 21 (1978).

[16]B. A. Weinstein and G. P. Piermarini, Phys. Lett. 48A, 14 (1974).

[17]R. Trommer, Ph.D. thesis, University of Stuttgart, 1977 (unpublished).